

PCNA function in the activation and strand direction of MutL α endonuclease in mismatch repair

Anna Pluciennik^{a,1}, Leonid Dzutiev^{a,1,3}, Ravi R. Iyer^a, Nicoleta Constantin^a, Farid A. Kadyrov^{a,4}, and Paul Modrich^{a,b,2}

^aDepartment of Biochemistry and ^bHoward Hughes Medical Institute, Box 3711, Duke University Medical Center, Durham, NC 27710

Contributed by Paul Modrich, July 22, 2010 (sent for review June 30, 2010)

MutL α (MLH1–PMS2) is a latent endonuclease that is activated in a mismatch-, MutS α -, proliferating cell nuclear antigen (PCNA)-, replication factor C (RFC)-, and ATP-dependent manner, with nuclease action directed to the heteroduplex strand that contains a preexisting break. RFC depletion experiments and use of linear DNAs indicate that RFC function in endonuclease activation is limited to PCNA loading. Whereas nicked circular heteroduplex DNA is a good substrate for PCNA loading and for endonuclease activation on the incised strand, covalently closed, relaxed circular DNA is a poor substrate for both reactions. However, covalently closed supercoiled or bubble-containing relaxed heteroduplexes, which do support PCNA loading, also support MutL α activation, but in this case cleavage strand bias is largely abolished. Based on these findings we suggest that PCNA has two roles in MutL α function: The clamp is required for endonuclease activation, an effect that apparently involves interaction of the two proteins, and by virtue of its loading orientation, PCNA determines the strand direction of MutL α incision. These results also provide a potential mechanism for activation of mismatch repair on nonreplicating DNA, an effect that may have implications for the somatic phase of triplet repeat expansion.

MutLalpha | genetic instability | cancer | triplet repeats

The best understood function of mismatch repair is its role in correction of replication errors, which requires that repair be directed to a newly synthesized DNA strand. A strand-specific nick or gap is sufficient to direct mismatch repair in extracts of mammalian and *Drosophila* cells, or in *Xenopus* egg extracts (1–4), and an obvious possibility is that DNA termini that occur naturally at the replication fork serve as the strand signals that direct the reaction in the eukaryotic cell. Whereas the strand break that directs in vitro repair can be located either 3' or 5' to the mismatch, only a single excision activity has been implicated in the eukaryotic reaction. Exonuclease 1 (Exo1), which hydrolyzes duplex DNA with 5' to 3' polarity, has been implicated in both yeast and mammalian mismatch repair, and in the latter case has been shown to function in both 3'- and 5'-directed repair events (1–4).

A possible explanation for this polarity paradox has been provided by analysis of a purified system comprised of MutS α (MSH2–MSH6 heterodimer), MutL α (MLH1–PMS2 heterodimer), the replication clamp proliferating cell nuclear antigen (PCNA), the clamp loader replication factor C (RFC), the single-stranded DNA binding protein replication protein A, Exo1 and DNA polymerase δ . Repair and mismatch-provoked excision in this minimal system recapitulate bidirectional features of the extract reaction, and as in extracts, Exo1 supports repair directed by either a 3' or 5' strand break (5, 6). This puzzling observation was clarified by the finding that eukaryotic MutL α is a latent endonuclease that is activated in a mismatch-, MutS α - (or MutS β -), PCNA-, RFC-, and ATP-dependent fashion in a reaction that also depends on presence of a preexisting break in one heteroduplex strand (7–9). Incision by activated MutL α is directed to the heteroduplex strand that contains a preexisting strand break and is biased to the distal side of the mismatch. For a 3' heteroduplex this results in incision 5' to the mismatch to yield a product in which

the mismatch is bracketed by strand breaks. Multiply incised molecules produced in this manner are substrates for MutS α -activated Exo1 (7, 10), which removes the DNA segment spanning the mismatch by 5' to 3' hydrolysis.

Although attempts to identify other exonucleases that function in eukaryotic mismatch repair have yielded negative results, eukaryotic cells support a significant level of Exo1-independent mismatch correction that accounts for 10–40% of the repair events that occur in mammalian cells (11, 12). A recent analysis of this effect has led to the suggestion that repair in the absence of Exo1 occurs via strand displacement synthesis by DNA polymerase δ in a reaction that depends on the introduction of secondary strand breaks by MutL α (13).

Although the endonuclease activity of MutL α plays a central role in the current understanding of eukaryotic mismatch correction, the mechanism of endonuclease activation and the factor(s) involved in strand direction of this activity are not known. The study described here addresses involvement of RFC, PCNA, and a DNA strand break in these effects.

Results

The Primary Function of RFC in MutL α Activation Is PCNA Loading. At physiological ionic strength in the presence of Mg²⁺, MutL α endonuclease activation requires a mismatch, MutS α (or MutS β), PCNA, RFC, and a strand break (7–9). MutS α /MutS β is required for mismatch recognition, but the individual roles of PCNA and RFC in this reaction have not been defined. PCNA interaction with MutL α has been demonstrated (5, 14, 15), suggesting that this interaction may play a role in endonuclease activation (8). However, it is unclear whether RFC function is restricted to clamp loading. We have addressed this issue using a set of near homogeneous proteins (Fig. S1). PCNA was loaded onto 3'-nicked G–T heteroduplex DNA and Superdex 200 gel filtration employed to resolve PCNA–DNA complexes from unbound protein. This procedure was facilitated by use of yeast RFC Δ N (yRFC Δ N; this designation will be used below to distinguish this activity from human RFC), which lacks the ligase homology domain of the large subunit and displays reduced DNA affinity (16), but nevertheless efficiently loads human PCNA onto nicked DNA and is functional in reconstituted human mismatch-provoked excision (5).

As shown in Fig. 1A and Fig. S2, the bulk of the DNA eluted from Superdex 200 in the column void volume in fractions 15–18, well separated from free yRFC Δ N and PCNA, which eluted in

Author contributions: A.P., L.D., R.R.I., N.C., F.A.K., and P.M. designed research; A.P., L.D., R.R.I., and N.C. performed research; A.P., L.D., R.R.I., N.C., and P.M. analyzed data; and A.P., L.D., and P.M. wrote the paper.

The authors declare no conflict of interest.

Freely available online through the PNAS open access option.

¹A.P. and L.D. contributed equally to this work.

²To whom correspondence should be addressed. E-mail: modrich@biochem.duke.edu.

³Present address: Meso Scale Discovery, 9238 Gaithersburg Road, Gaithersburg, MD 20877.

⁴Present address: Department of Biochemistry and Molecular Biology, Southern Illinois University School of Medicine, Carbondale, IL 62901.

This article contains supporting information online at www.pnas.org/lookup/suppl/doi:10.1073/pnas.1010662107/-DCSupplemental.

fractions 25–31. Western blot analysis of column fractions (Fig. S2B) demonstrated that PCNA coeluted with DNA in fractions 15–18 with an efficiency of clamp loading of about 4 PCNA

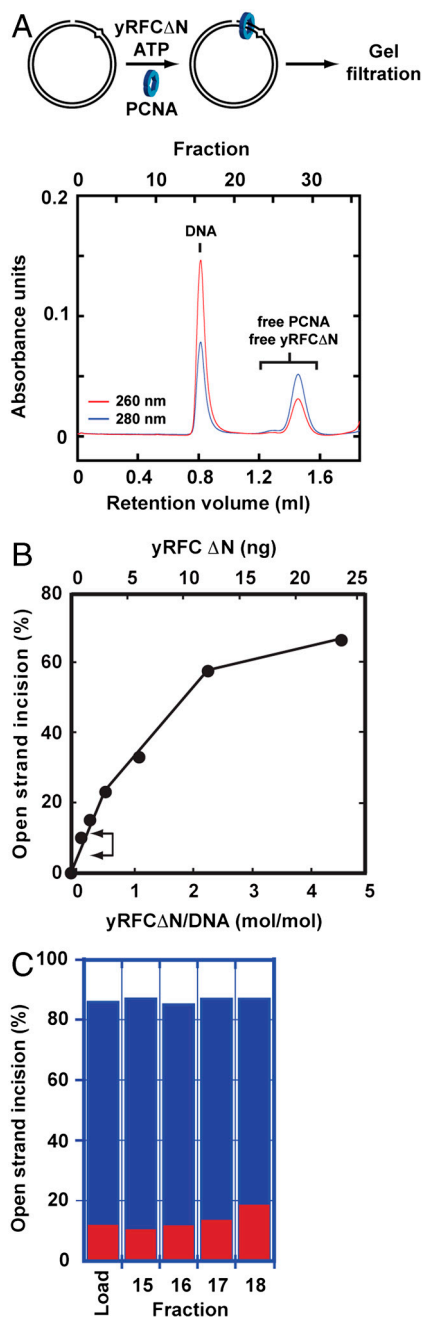


Fig. 1. RFC function in MutL α activation is limited to PCNA loading. (A) Human PCNA was loaded onto 3' G-T heteroduplex DNA using yRFC Δ N, and reaction products subjected to Superdex 200 gel filtration (*Materials and Methods*). DNA eluted in fractions 15–18 and unbound protein in fractions 25–31. (B) The yRFC Δ N dependence of MutL α endonuclease activation was determined using 24 fmol 3' G-T heteroduplex DNA as described in *Materials and Methods*. Values shown are corrected for a modest background level of random strand breaks in the heteroduplex preparation used. The bracket indicates the activity range supported by the yRFC Δ N levels present in 10 μ L of Superdex 200 fractions 15–18 as estimated by Western blot (Fig. S2B). (C) Ten μ L of the indicated Superdex 200 fractions were assayed for strand-directed endonuclease activity in the absence (red bars) or presence of MutS α and MutL α [blue bars (*Materials and Methods*), mismatch-dependent conditions]. Background strand breaks in the heteroduplex preparation used were comparable to those observed when MutS α and MutL α were omitted from the incubation (red bars). Raw data for this analysis is shown in Fig. S2A.

trimers per heteroduplex. However, these fractions contained only trace amounts of yRFC Δ N, levels sufficient to support MutL α activation at only 5–11% of the maximal level (Fig. 1B, bracket). Nevertheless, supplementation of samples of these fractions with MutS α and MutL α resulted in robust endonuclease activation (>70% cleavage, Fig. 1C), with incision directed to nicked heteroduplex strand (Fig. S2A). These findings suggest that yRFC Δ N function in MutL α activation is restricted to clamp loading.

Further support for this idea was provided by analysis of MutL α endonuclease on linear homoduplex DNA. We have previously shown that constitutive endonuclease activity can be demonstrated in MutL α preparations provided the ionic strength is low and Mn²⁺ is substituted for Mg²⁺. The Mn²⁺-dependent activity does not respond to MutS α , but is strongly stimulated on the incised strand of nicked circular DNA by PCNA and RFC, and both proteins are required for this effect (7, 8). Fig. 2A demonstrates that incision of a linear 202 bp duplex by the Mn²⁺-dependent nuclease is also dramatically activated in the presence of yRFC Δ N and PCNA (compare lanes 1 and 3), but in contrast to results with nicked circular DNA, PCNA alone is sufficient to account for the MutL α activation observed (compare lanes 2 and 3). The RFC independence of this linear DNA effect is reminiscent of RFC-independent PCNA activation of DNA polymerase δ on linear template-primers (17), and provides additional support for the idea that RFC function in MutL α endonuclease activation is restricted to loading of PCNA onto DNA to which it is otherwise topologically inaccessible. The fact that PCNA is sufficient to activate MutL α in this system indicates that interaction of the two proteins, presumably while DNA-bound, is required for this effect. Consistent with this idea is the finding that PCNA activation of MutL α in this two-protein system is blocked by a peptide containing the p21 PCNA interaction motif, which interferes with a number of PCNA-dependent processes (18), but not by a scrambled sequence peptide (Fig. S3A).

Mismatch- and RFC-Independent but PCNA- and MutS α -Dependent Activation of MutL α . The simplified Mn²⁺-dependent mismatch-independent reaction described above has partially clarified PCNA function in MutL α activation. By manipulating reaction components, we have also sought conditions where MutL α acti-

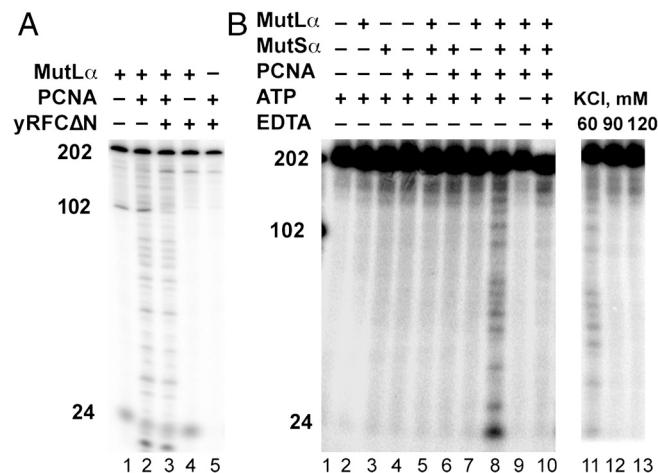


Fig. 2. Endonuclease activity on linear DNA requires PCNA but not RFC. Mismatch-independent MutL α endonuclease activity on 202 bp linear homoduplex DNA as described in *Materials and Methods* in the presence of reaction components as indicated. (A) Reactions contained 30 mM KCl, 0.5 mM ATP, 1 mM MnSO₄, and protein components as indicated. (B) Reactions contained 60 mM KCl, 1.5 mM ATP, 5 mM MgCl₂, and indicated proteins. ATP was omitted from the reaction in lane 8 and EDTA substituted for MgCl₂ in lane 9. Reactions shown in lanes 11–13 were performed as for lane 8 except that final KCl concentration was varied as shown.

vation depends on both PCNA and MutS α , but is independent of RFC and a mismatched base pair. As shown in Fig. 2B (lanes 1–10), a neutral pH buffer containing 60 mM KCl and 5 mM MgCl₂ is sufficient in this regard. Under these conditions, MutL α activation requires MutS α , PCNA, ATP, and a divalent cation, but is independent of RFC and mismatch. Inasmuch as PCNA–MutS α interaction is not necessary for MutL α activation (19), we infer that the MutS α requirement for this reduced-specificity reaction reflects a requirement for MutS α –MutL α interaction. Endonuclease activation in this manner was abolished when the KCl concentration was increased to physiological levels that are employed for study of mismatch-dependent activation of MutL α (120–125 mM; Fig. 2B [lanes 11–13, (7)]).

The observed distributions of cleavage sites within the 202 bp homoduplex under MutS α -independent and MutS α -dependent conditions were similar, and in both cases were nonrandom (Figs. 2A and B). Furthermore, the distribution of incision sites relative to labeled 5'-termini differed for the two strands of the homoduplex (Fig. S3B), suggesting that MutL α incision responds to some extent to sequence context.

Loaded PCNA on a Supercoiled Heteroduplex Is Sufficient to Activate MutL α Nuclease in a MutS α -Dependent Manner, but Incision Occurs Without Strand Bias. At physiological ionic strength in the presence of Mg²⁺, activation of MutL α endonuclease requires a mismatch, MutS α , PCNA, RFC, and depends on the presence of a single strand interruption within the heteroduplex (7, 8). In addition to its involvement in MutL α activation, the strand break also determines the strand-specificity of incision by the activated endonuclease. One probable function of the strand discontinuity is provision of a loading site for PCNA (20, 21), and it has been suggested that loaded PCNA may function as an effector for communication between the strand break and mismatch for the purpose of strand discrimination (8, 14). To evaluate potential involvement of PCNA in strand discrimination, we have sought conditions that support PCNA loading onto closed circular DNA.

RFc has been shown to load PCNA onto closed circular DNA at low ionic strength, with negatively supercoiled molecules being better substrates than relaxed circles (20), and similar results have been obtained with the *Escherichia coli* β clamp and the γ complex clamp loader (22). It has been suggested that loading onto supercoiled DNA is due to transient helix opening driven by the free energy of supercoiling and the consequent production of double strand-single strand junctions that serve as sites for clamp assembly (22). To evaluate PCNA loading onto circular heteroduplex DNAs, we utilized a PCNA variant that can be ³²P-labeled coupled with gel filtration assay to score loading of clamps onto the helix (refs. 20 and 23 and Fig. S4). As summarized in the second column of Fig. 3A and B, RFC and yRFC Δ N are capable of loading PCNA onto supercoiled heteroduplex DNA at physiological salt concentration (125 mM NaCl, 5 mM MgCl₂). In fact, the efficiency of PCNA loading by yRFC Δ N onto a supercoiled G–T heteroduplex (6 clamps/DNA) is similar to that observed with the nicked substrate (4 clamps/DNA). As expected, human RFC also efficiently loaded PCNA onto nicked DNA (7 clamps/DNA), but was less effective than yRFC Δ N with the supercoiled heteroduplex (2 clamps/DNA). Relaxed closed circular heteroduplex was the weakest substrate for clamp loading under these conditions (1 clamp per heteroduplex). Our results with supercoiled DNA differ somewhat from those of Podust et al. (20), who found that RFC loading of PCNA onto supercoils is greatly reduced at physiological salt concentration. We attribute this difference to the fact that the supercoiled heteroduplexes used in our studies were prepared to have approximately twice the superhelical density of plasmid DNA isolated from *E. coli* (Materials and Methods) to facilitate helix opening at elevated ionic strength.

We thus asked whether the ability of yRFC Δ N and RFC to load PCNA onto negatively supercoiled heteroduplex DNA bypasses the requirement for a strand break in MutL α activation. Fig. 3 (columns 7 and 9) summarizes the efficiencies of MutL α activation for several G–T heteroduplex and control A–T homoduplex DNAs as a function of strand break status and tertiary conformation. As observed previously (7), MutL α incision of nicked heteroduplex DNA requires a mismatch, MutS α , PCNA, and RFC (or yRFC Δ N), and is strongly biased to the heteroduplex strand that contains a preexisting break. However, an otherwise identical relaxed closed circular heteroduplex was found to be inert as substrate, with levels of incision similar to those obtained with nicked or supercoiled homoduplex controls. By contrast, the negatively supercoiled G–T heteroduplex does support mismatch-dependent MutL α endonuclease activation with the same protein requirements as those for a nicked heteroduplex, but incision of the superhelical substrate occurs with minimal strand bias (Fig. 3A and B). The implications of this finding will be considered below.

Although RFC and yRFC Δ N support comparable levels of MutL α activation on nicked heteroduplex DNA, yRFC Δ N was consistently found to provide higher levels of activation with a superhelical heteroduplex (Fig. 3A and B), an effect that correlates with the differential ability of the two activities to load PCNA onto negatively supercoiled DNA. This effect and an empirical comparison of the efficiency of MutL α activation as a function of the extent of PCNA loading by RFC and yRFC Δ N are illustrated in Fig. 4. For a given extent of PCNA loading, reactions containing native human RFC resulted in a somewhat reduced level of MutL α activation as compared to that observed with yRFC Δ N. Although we have not established the basis for this effect, it is known that native RFC avidly binds to DNA, an effect that is abrogated by deletion of the ligase homology domain of the large subunit as in yRFC Δ N (16). It is possible that the modest activity reduction observed with native RFC is the result of inhibition by the DNA-bound protein.



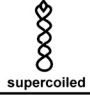
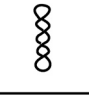


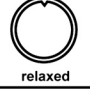
Relaxed, Bubble-Containing Heteroduplex DNA Supports PCNA Loading and MutL α Activation, but Incision Occurs Without Strand Bias. Clamp loading onto supercoiled DNA has been postulated to occur at transient double strand-single strand junctions that result from helix breathing events driven by the free energy of supercoiling (22). To directly test whether double strand-single strand junctions within a covalently continuous duplex can provide PCNA loading sites, we prepared a relaxed closed circular G–T heteroduplex that contains a 10 bp bubble comprised of a *d*(T)₁₀ sequence within each strand. Unlike simple relaxed circular heteroduplex DNA, the bubble-containing heteroduplex does support efficient PCNA loading by both RFC and yRFC Δ N (Fig. 3 and Fig. S4). Furthermore, like supercoiled heteroduplex DNA, the bubble-containing relaxed substrate supports mismatch-, MutS α -, PCNA- and RFC/yRFC Δ N-dependent activation of MutL α endonuclease (Fig. 3). As in the case of supercoiled substrate, incision of the bubble-containing relaxed heteroduplex occurs with limited strand bias.

Bubble-containing A–T control DNA was subject to incision at 50 to 70% the efficiency observed with the bubble-containing G–T heteroduplex, and this occurred without significant strand bias. Because incision in this manner was MutS α -dependent (Fig. S5), we attribute this effect to bubble recognition by the MSH2–MSH6 heterodimer, a finding consistent with the demonstration that MutS α is capable of recognizing heterologies involving multiple unpaired nucleotides (1).

Discussion

This study addresses the functions of RFC, PCNA, and the heteroduplex strand break in the activation and strand direction of the MutL α endonuclease. Our results strongly suggest that RFC

A

			Endonucleolytic incision (fmol/10 min)					
Heteroduplex	Loaded PCNA trimer/DNA	Strand	PCNA MutL α	PCNA RFC MutL α	PCNA MutL α MutS α	PCNA RFC MutL α MutS α	Homoduplex	PCNA RFC MutL α MutS α
 nicked	7.0 ± 0.2	C (nicked)	0.2 ± 0.1	0.5 ± 0.5*	0.7 ± 0.2	14 ± 2.3		1.2 ± 0.8
		V (closed)	0.9 ± 0.4	1.2 ± 1*	1.8 ± 0.8	1.4 ± 1.5		0.9 ± 0.6
 supercoiled	2.1 ± 0.3	C (closed)	0.9 ± 0.5	0.7 ± 0.7*	1.2 ± 0.6	2.7 ± 1.1		0.5 ± 0.5
		V (closed)	0.9 ± 0.7	1.0 ± 0.8*	1.2 ± 0.4	3.8 ± 0.6		0.6 ± 0.2
 relaxed-bubble	3.9 ± 0.1	C (closed)	0.3 ± 0.4	0.4 ± 0.4	0.8 ± 0.6	2.9 ± 0.2		1.9 ± 0.1*
		V (closed)	0.4 ± 0.4	0.8 ± 0.4	1.0 ± 0.7	5.1 ± 1.3		2.0 ± 0.3*
 relaxed	1.2 ± 0.6	C (closed)	0.7 ± 0.5	0.5 ± 0.4	0.4 ± 0.2	0.6 ± 0.5		
		V (closed)	0.7 ± 1	0.2 ± 0.3	0.4 ± 0.6	0.7 ± 0.6		

B



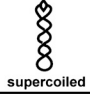




			Endonucleolytic incision (fmol/10 min)					
Heteroduplex	Loaded PCNA trimer/DNA	Strand	PCNA MutL α	PCNA yRFC Δ N MutL α	PCNA MutL α MutS α	PCNA yRFC Δ N MutL α MutS α	Homoduplex	PCNA yRFC Δ N MutL α MutS α
 nicked	4.4 ± 0.1	C (nicked)	0.2 ± 0.1	1.1 ± 1.5*	0.7 ± 0.2	14 ± 0.3		1.7 ± 0.4
		V (closed)	0.9 ± 0.4	1.5 ± 2*	1.8 ± 0.8	3.3 ± 0.5		1.1 ± 0.3
 supercoiled	6 ± 1.4	C (closed)	0.9 ± 0.5	1.1 ± 0.5*	1.2 ± 0.6	7.4 ± 1		1.6 ± 1.1
		V (closed)	0.9 ± 0.7	0.5 ± 0.6*	1.2 ± 0.4	10 ± 0.6		1.9 ± 1.1
 relaxed-bubble	4.2 ± 0.1	C (closed)	0.3 ± 0.4	0.7 ± 0.8	0.8 ± 0.6	6.6 ± 1.1		5.8 ± 1.4
		V (closed)	0.4 ± 0.4	0.9 ± 1.1	1.0 ± 0.7	9.6 ± 1.8		5.3 ± 2.4
 relaxed	1.2 ± 0.1	C (closed)	0.7 ± 0.5	0.6 ± 0.4	0.4 ± 0.2	1.1 ± 0.5		
		V (closed)	0.7 ± 1	0.6 ± 0.8	0.4 ± 0.6	1.0 ± 0.7		

Fig. 3. Strand break and DNA topology dependence of PCNA loading and MutL α activation. Efficiency of PCNA loading onto nicked, supercoiled ($\sigma = -0.12$), relaxed bubble, and relaxed G-T heteroduplexes was determined by gel filtration assay (*Materials and Methods* and Fig. S4). Loading values shown are corrected for that observed in the absence of ATP (0.5 PCNA trimer/DNA). Clamp loading utilized native human RFC (A) or yRFC Δ N (B). For supercoiled DNA, loading values are the mean of 3 determinations (± 1 standard deviation); for other DNAs, values are the average of 2 determinations, with the variation shown corresponding to the range observed. MutL α endonucleolytic incision of complementary (C) and viral (V) strands of these heteroduplexes (or A-T homoduplex controls) was determined in the presence of the indicated proteins and quantified as described under *Materials and Methods*, and corrected for presence of background nicks in DNA preparations as described in Fig. 1. Incision values indicated with an asterisk are the average of 2 determinations, with the range observed indicated. Other values are the mean of 3 to 6 determinations \pm one standard deviation.

function in this reaction is restricted to PCNA loading and that MutL α -clamp interaction is required for endonuclease activation. We have also found that the requirement for a strand break in MutL α activation can be bypassed by DNA structural anomalies within a covalently closed circular heteroduplex that provide sites for PCNA loading. In contrast to MutL α action on nicked circular heteroduplex DNA, where incision is directed to the strand containing a preexisting break, incision of these closed circular substrates targets both DNA strands.

These findings, coupled with a previous analysis of mismatch-independent MutL α incision of nicked circular homoduplex DNA in the presence of low salt and Mn $^{2+}$, have led us to the model for MutL α action shown in Fig. 5. In the presence of Mn $^{2+}$ but in the absence of other proteins, MutL α incises the nicked and continuous strands of nicked circular DNA at the same rate (8). Although without effect on the rate of incision of the continuous strand, supplementation with both RFC and

PCNA dramatically activates Mn $^{2+}$ -dependent incision of the strand with a preexisting nick. Based on the results described here, we attribute this effect to PCNA loading. The β and PCNA sliding clamps are loaded at a 3' double strand-single strand junction (24). The two faces of each of these clamps are nonequivalent (18, 25), and available evidence indicates that they are loaded onto DNA with a specific orientation relative to that of the 3' double strand-single strand junction (refs. 26 and 27 and Fig. 5A). We thus propose that the asymmetry of the loaded clamp is manifested in the PCNA-MutL α complex, and that this asymmetry directs the strand-specificity of MutL α action. Interaction of MutL α with a particular face of the clamp is consistent with our finding that PCNA activation of MutL α in the presence of Mn $^{2+}$ is blocked by p21 peptide (Fig. S3A), which preferentially interacts with one side of the clamp (18). Because PCNA can diffuse along DNA (28), the asymmetry conferred during clamp loading

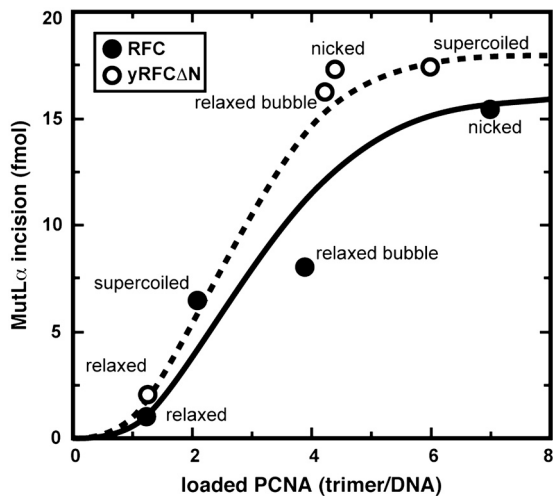


Fig. 4. MutL α activation as a function of extent of PCNA loading. Extents of MutL α activation are plotted against efficiencies of PCNA loading by RFC and yRFC Δ N for the heteroduplexes shown in Fig. 3. Lines shown are empirical fits.

could be carried along the helix to dictate the strand-specificity of MutL α action elsewhere on the DNA.

This model accounts for the mismatch-dependent results we have obtained with supercoiled DNA and relaxed bubble-containing heteroduplexes. Clamp loading onto negatively super-twisted DNA has been postulated to occur at double strand-single strand junctions that result from transient helix opening (22). We have shown that a short region of open helix within a relaxed circular duplex does indeed provide a target for PCNA loading. An open region of helix has two double strand-single strand junctions, and these are rotationally symmetric, implying that such structures must support the loading of PCNA in both orientations relative to the absolute orientation of the duplex (Fig. 5B). Consequently, PCNA loaded onto supercoiled or a relaxed bubble-containing heteroduplex would be expected to activate MutL α cleavage of both DNA strands, which is what we have observed.

The process of MutL α endonuclease activation displays strong apparent cooperativity with respect to the number of PCNA clamps present on the circular heteroduplexes used in this study (Fig. 4). There are two types of explanation for this observation. Activation of the endonuclease could involve MutL α interaction with several clamps or the assembly of a higher order complex involving multiple molecules of both MutL α and PCNA. We regard such mechanisms as unlikely because the dependence of endonuclease activation on MutL α concentration is not cooperative (7). A second possibility is that the PCNA cooperativity observed is an apparent effect that is not actually manifested at the level of the mechanism. For example, whereas MutL α is recruited by MutS α to the vicinity of the mismatch (29), loaded PCNA is free to diffuse along the helix (28). The loading of multiple clamps onto the 6,400 bp heteroduplex used in our experiments may thus be required simply to achieve a local PCNA concentration that is sufficient to activate MutL α . We favor this sort of explanation for the cooperativity observed in Fig. 4.

In addition to clarifying the nature of MutL α activation, the findings described here may have implications for the expansion of (CAG) $_n$:(CTG) $_n$ triplet repeat sequences, the cause of a number of neurodegenerative diseases (30, 31). Somatic expansion, which depends on both MutS β and MutL α has been attributed to processing of strand slippage products, with the probability of such slippage events increasing with repeat number (31, 32). However, such expansions have been shown to occur in postmitotic neurons (33) in the absence of DNA replication. This finding is puzzling because previous work on both bacterial and eukaryotic

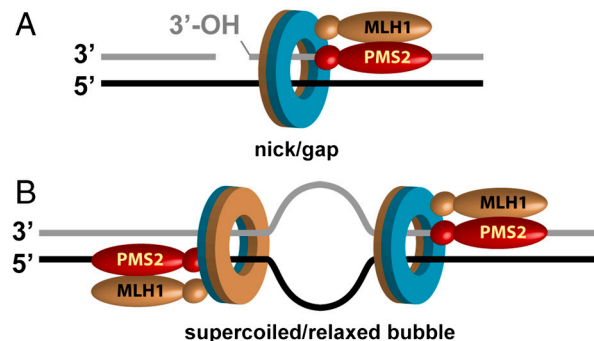


Fig. 5. Model for PCNA involvement in the strand direction of MutL α endonuclease. As indicated by blue and tan colors, the two faces of PCNA are nonequivalent, and the clamp is loaded with a unique orientation relative to the 3' double strand-single strand junction at a nick or gap (A). A transient (22) or artificial bubble (this study) within a covalently closed circular DNA also supports clamp loading. Because the double strand-single strand junctions at the two ends of a bubble are rotationally symmetric, such structures must support PCNA loading in either orientation (B). We suggest that the MutL α -PCNA complex is characterized by intrinsic asymmetry and that this asymmetry coupled with PCNA loading orientation dictates the strand specificity of incision by the MutL α endonuclease active site within the PMS2 subunit.

mismatch correction has indicated a requirement for a strand break to initiate excision repair (1–4). We have shown here that DNA strand break involvement in the human repair reaction is restricted to provision of a loading site for PCNA, and that the strand break requirement can be bypassed if an alternate clamp loading site is available; e.g. a small bubble within a covalently continuous heteroduplex. It is thus plausible that extruded (CAG) $_x$ and/or (CTG) $_x$ elements resulting from strand slippage within a nonreplicating (CAG) $_n$:(CTG) $_n$ repeat could provide not only a MutS β -recognizable lesion, but a PCNA loading site as well, which would lead to functional activation of the repair system on nonreplicating DNA. We are pursuing this possibility.

Materials and Methods

Proteins and DNAs. Proteins, DNAs, and Western blot procedures used in this study are described in *SI Text*.

PCNA Loading Assay. PK-PCNA was radiolabeled at 30 °C for 30 min in 30 μ L reactions containing 20 μ g PK-PCNA, 20 mM Tris-HCl pH 7.5, 60 μ Ci [γ - 32 P]ATP (6000 Ci/mmol), 13 μ M cold ATP, 10 mM MgCl $_2$, 17 mM NaCl, 0.4 mM DTT and 500 units of cAMP-dependent protein kinase catalytic subunit (New England Biolabs) (20, 23). Free ATP was removed by filtration through a Quick Spin Sephadex G-50 column (Roche). Specific activities of preparations ranged from 1×10^5 to 3×10^5 cpm/pmol trimer. [32 P]PK-PCNA loading reactions (20 μ L) contained 20 mM Tris-HCl, pH 7.6, 125 mM NaCl, 5 mM MgCl $_2$, 1.5 mM ATP, 1 mM glutathione, 0.05 mg/mL BSA, 100–140 fmol DNA, 2100 fmol [32 P]PK-PCNA homotrimer, 620 fmol RFC or 820 fmol yRFC Δ N. After incubation at 37 °C for 3 min, the reaction was chilled on ice and 10 μ L was loaded onto a 3.2 \times 300 mm Superdex 200 column (GE Healthcare) equilibrated with 20 mM Tris-HCl, pH 7.6, 125 mM NaCl, 5 mM MgCl $_2$, 1 mM EDTA, 1 mM DTT at 95 μ L/min at 4 °C. The column eluate was monitored at 260 and 280 nm. Extent of [32 P]PK-PCNA loading was determined by liquid scintillation counting.

Preparative PCNA loading reactions (70 μ L) for isolation of PCNA-DNA complexes contained 20 mM Tris-HCl, pH 7.6, 125 mM NaCl, 5 mM MgCl $_2$, 1.5 mM ATP, 1 mM glutathione, 336 fmol nicked circular 3' G-T heteroduplex DNA, 10 pmol PCNA trimer and 1.9 pmol yRFC Δ N. After incubation at 37 °C for 3 min, reactions were chilled on ice. Two-5 μ L samples were removed, adjusted to 10 μ L with 20 mM Tris-HCl, pH 7.6, 125 mM NaCl, 5 mM MgCl $_2$, 1 mM EDTA and 1 mM DTT, and scored for endonuclease activity as described below in 20 μ L reactions in the absence or presence of 390 fmol MutS α and 460 fmol MutL α . Fifty μ L of the remainder was loaded onto a Superdex 200 column and chromatographed as described above and 52 μ L fractions collected. Twenty μ L samples were analyzed by immunoblot for presence of yRFC Δ N and PCNA (*SI Text*). Ten μ L samples of fractions 14–18 containing DNA were supplemented with 10 μ L of 20 mM Tris-HCl, pH 7.6, 125 mM NaCl, 5 mM MgCl $_2$, 3 mM

ATP, 2 mM glutathione, 0.1 mg/mL BSA, 8% vol/vol glycerol containing 390 fmol MutS α , and 460 fmol MutL α . After incubation for an additional 10 min at 37 °C, reactions were stopped with 5 μ L of 0.3 M NaOH, 0.1 M EDTA and analyzed by southern hybridization as described below.

MutL α Endonuclease Assays. Mismatch-dependent MutL α endonuclease activation assay was performed by a modification of that used previously (7). Reactions (10 μ L) contained 20 mM Tris-HCl, pH 7.6, 125 mM KCl, 5 mM MgCl₂, 1.5 mM ATP, 1 mM glutathione, 0.05 mg/mL BSA, 4% vol/vol glycerol, 24 fmol DNA as indicated, 580 fmol PCNA trimer, and unless indicated otherwise, 100 fmol RFC or 136 fmol yRFC Δ N. After 10 min at 37 °C, 10 μ L of a solution containing 390 fmol MutS α , and 460 fmol MutL α in the same buffer were added. After incubation for an additional 10 min, reactions were terminated by addition of 40 μ L of 30 mM EDTA, 180 μ g/mL proteinase K and 0.4 mg/mL glycogen. After 20 min at 55 °C, reactions were phenol extracted, and DNA ethanol precipitated and digested with ClaI. Alternatively, reactions were terminated with 5 μ L of 0.3 M NaOH, 0.1 M EDTA. DNA products were resolved by electrophoresis through alkaline agarose, transferred to Hybond membrane, and the two strands detected by indirect end labeling with ³²P-labeled oligonucleotides V5504, V2505 (for DNAs digested with ClaI)

or C2526, corresponding to f1 viral strand coordinates 5504–5523 (d(ATCATTAAGCGCGCGGGTG)) or 2505–2526, or complementary strand coordinates 2505–2526, respectively (5).

Mismatch-independent MutL α endonuclease activity was determined in 10 μ L reactions containing 20 mM Tris-HCl, pH 7.6, 100 fmol 200 or 202 bp homoduplex DNA (5'-³²P labeled on one strand) in the presence of salt, ATP, divalent cation, MutS α (780 fmol), MutL α (1,700 fmol), PCNA (2,300 fmol, trimer) and yRFC Δ N (470 fmol) as indicated. After incubation at 37 °C for 20 min, reactions were stopped with 90% formamide and products resolved by electrophoresis through 8% polyacrylamide gels containing 8 M urea in 45 mM Tris-borate, 1 mM EDTA, pH 8.0, followed by phosphorimaging.

ACKNOWLEDGMENTS. We thank Bruce Stillman, Peter Burgers, and Mike O'Donnell for expression plasmids, Hongbing Shao for chromatography assistance, Elisabeth Penland for tissue culture support, and Tao-shih Hsieh for suggesting the bubble heteroduplex experiment. This work was supported in part by National Institutes of Health Grants R01 GM45190 and P01 CA092584. P.M. is an investigator of the Howard Hughes Medical Institute.

- Iyer RR, Pluciennik A, Burdett V, Modrich PL (2006) DNA mismatch repair: functions and mechanisms. *Chem Rev* 106:302–323.
- Modrich P (2006) Mechanisms in eukaryotic mismatch repair. *J Biol Chem* 281:30305–30309.
- Jiricny J (2006) The multifaceted mismatch-repair system. *Nat Rev Mol Cell Biol* 7:335–346.
- Hsieh P, Yamane K (2008) DNA mismatch repair: Molecular mechanism, cancer, and ageing. *Mech Ageing Dev* 129:391–407.
- Dzantiev L, et al. (2004) A defined human system that supports bidirectional mismatch-provoked excision. *Mol Cell* 15:31–41.
- Constantin N, Dzantiev L, Kadyrov FA, Modrich P (2005) Human mismatch repair: Reconstitution of a nick-directed bidirectional reaction. *J Biol Chem* 280:39752–39761.
- Kadyrov FA, Dzantiev L, Constantin N, Modrich P (2006) Endonucleolytic function of MutL α in human mismatch repair. *Cell* 126:297–308.
- Kadyrov FA, et al. (2007) *Saccharomyces cerevisiae* MutL α is a mismatch repair endonuclease. *J Biol Chem* 282:37181–37190.
- Iyer RR, et al. (2010) MutL α and proliferating cell nuclear antigen share binding sites on MutS β . *J Biol Chem* 285:11730–11739.
- Genschel J, Modrich P (2003) Mechanism of 5'-directed excision in human mismatch repair. *Mol Cell* 12:1077–1086.
- Genschel J, Bazemore LR, Modrich P (2002) Human exonuclease I is required for 5' and 3' mismatch repair. *J Biol Chem* 277:13302–13311.
- Wei K, et al. (2003) Inactivation of Exonuclease 1 in mice results in DNA mismatch repair defects, increased cancer susceptibility, and male and female sterility. *Genes Dev* 17:603–614.
- Kadyrov FA, et al. (2009) A possible mechanism for exonuclease 1-independent eukaryotic mismatch repair. *Proc Natl Acad Sci USA* 106:8495–8500.
- Umar A, et al. (1996) Requirement for PCNA in DNA mismatch repair at a step preceding DNA resynthesis. *Cell* 87:65–73.
- Lee SD, Alani E (2006) Analysis of interactions between mismatch repair initiation factors and the replication processivity factor PCNA. *J Mol Biol* 355:175–184.
- Gomes XV, Gary SL, Burgers PM (2000) Overproduction in *Escherichia coli* and characterization of yeast replication factor C lacking the ligase homology domain. *J Biol Chem* 275:14541–14549.
- Podust VN, Chang LS, Ott R, Dianov GL, Fanning E (2002) Reconstitution of human DNA polymerase δ using recombinant baculoviruses: The p12 subunit potentiates DNA polymerizing activity of the four-subunit enzyme. *J Biol Chem* 277:3894–3901.
- Gulbis JM, Kelman Z, Hurwitz J, O'Donnell M, Kuriyan J (1996) Structure of the C-terminal region of p21(WAF1/CIP1) complexed with human PCNA. *Cell* 87:297–306.
- Iyer RR, et al. (2008) The MutS α -proliferating cell nuclear antigen interaction in human DNA mismatch repair. *J Biol Chem* 283:13310–13319.
- Podust LM, Podust VN, Sogo JM, Hubscher U (1995) Mammalian DNA polymerase auxiliary proteins: analysis of replication factor C-catalyzed proliferating cell nuclear antigen loading onto circular double-stranded DNA. *Mol Cell Biol* 15:3072–3081.
- Cai J, et al. (1996) Reconstitution of human replication factor C from its five subunits in baculovirus-infected insect cells. *Proc Natl Acad Sci USA* 93:12896–12901.
- Yao N, Leu FP, Anjelkovic J, Turner J, O'Donnell M (2000) DNA structure requirements for the *Escherichia coli* gamma complex clamp loader and DNA polymerase III holoenzyme. *J Biol Chem* 275:11440–11450.
- Kelman Z, Naktinis V, O'Donnell M (1995) Radiolabeling of proteins for biochemical studies. *Method Enzymol* 262:430–442.
- Yao N, Hurwitz J, O'Donnell M (2000) Dynamics of beta and proliferating cell nuclear antigen sliding clamps in traversing DNA secondary structure. *J Biol Chem* 275:1421–1432.
- Kong XP, Onrust R, O'Donnell M, Kuriyan J (1992) Three-dimensional structure of the beta subunit of *E. coli* DNA polymerase III holoenzyme: A sliding DNA clamp. *Cell* 69:425–437.
- Bowman GD, O'Donnell M, Kuriyan J (2004) Structural analysis of a eukaryotic sliding DNA clamp-clamp loader complex. *Nature* 429:724–730.
- Georgescu RE, et al. (2008) Structure of a sliding clamp on DNA. *Cell* 132:43–54.
- Yao N, et al. (1996) Clamp loading, unloading and intrinsic stability of the PCNA, beta and gp45 sliding clamps of human, *E. coli* and T4 replicases. *Genes Cells* 1:101–113.
- Blackwell LJ, Wang S, Modrich P (2001) DNA chain length dependence of formation and dynamics of hMutS α -hMutL α -heteroduplex complexes. *J Biol Chem* 276:33233–33240.
- Brouwer JR, Willemsen R, Oostra BA (2009) Microsatellite repeat instability and neurological disease. *Bioessays* 31:71–83.
- Lopez Castel A, Cleary JD, Pearson CE (2010) Repeat instability as the basis for human diseases and as a potential target for therapy. *Nat Rev Mol Cell Biol* 11:165–170.
- Gomes-Pereira M, Fortune MT, Ingram L, McAbney JP, Monckton DG (2004) Pms2 is a genetic enhancer of trinucleotide CAG. CTG repeat somatic mosaicism: Implications for the mechanism of triplet repeat expansion. *Hum Mol Genet* 13:1815–1825.
- Gonitler R, et al. (2008) DNA instability in postmitotic neurons. *Proc Natl Acad Sci USA* 105:3467–3472.